Available online at www.sciencedirect.com
SCIENCE DIRECT®
Virology 322 (2004) 135–142
VIROLOGY
www.elsevier.com/locate/yviro

The C-terminal domain of the pVP2 precursor is essential for the interaction between VP2 and VP3, the capsid polypeptides of infectious bursal disease virus

Ana Oña,[a,1] Daniel Luque,[a,b] Fernando Abaitua,[a] Antonio Maraver,[a,2] José R. Castón,[b] and Jose F. Rodríguez[a,*]

[a] *Department of Biología Molecular y Celular, Centro Nacional de Biotecnología, Cantoblanco, 28049 Madrid, Spain*
[b] *Department of Estructura de Macromoléculas, Centro Nacional de Biotecnología, Cantoblanco, 28049 Madrid, Spain*

Received 10 November 2003; returned to author for revision 22 January 2004; accepted 22 January 2004

Abstract

The interaction between the infectious bursal disease virus (IBDV) capsid proteins VP2 and VP3 has been analyzed in vivo using baculovirus expression vectors. Data presented here demonstrate that the 71-amino acid C-terminal-specific domain of pVP2, the VP2 precursor, is essential for the establishment of the VP2–VP3 interaction. Additionally, we show that coexpression of the pVP2 and VP3 polypeptides from independent genes results in the assembly of virus-like particles (VLPs). This observation demonstrates that these two polypeptides contain the minimal information required for capsid assembly, and that this process does not require the presence of the precursor polyprotein.

Keywords: IBDV; Birnavirus; Capsid; Assembly; Polyprotein; Virus-like particle

Introduction

Infectious bursal disease virions are non-enveloped icosahedra (T = 13 symmetry) of 65–70 nm enclosing a bipartite dsRNA genome (Leong et al., 2000). According to 3D models (Böttcher et al., 1997; Castón et al., 2001; Lombardo et al., 1999), the infectious bursal disease virus (IBDV) capsid is a single protein layer formed by two polypeptides, VP2 (48 kDa) and VP3 (29 kDa). The external surface is a continuous lattice built up by 260 VP2 trimers. Associated to the inner surface of the VP2 lattice are at least 200 trimers of VP3. In addition to VP2 and VP3, the virus particle contains the putative virus-encoded RNA-dependent RNA polymerase (VP1) (Gorbalenya and Kooning, 1988; Müller and Nitschke, 1987). VP2 and VP3 are generated from a 109-kDa polyprotein in a process involving two independent proteolytic events. First, the polyprotein is autocatalytically processed releasing three polypeptides, pVP2, VP4, and VP3 (Kibenge et al., 1988). Thereafter, the pVP2 precursor undergoes a second proteolytic event that removes a 71-amino acid stretch, termed as pVP2-specific C-terminal domain (pVP2CTD), from its C-terminal end (Da Costa et al., 2002). pVP2CTD cleavage is subsequent to capsid assembly (Chevalier et al., 2002). Mutations near or within the pVP2CTD either reduce or arrest virus replication (Da Costa et al., 2002). The pVP2CTD regulates the assembly of pVP2 trimers (Castón et al., 2001). Hence, individual expression of pVP2 and VP2 yields different structural assemblages. While pVP2 self-assembles into irregular tubules, apparently formed by hexamers of pVP2 trimers, VP2 expression renders 23-nm capsid-like structures made up exclusively by pentamers of VP2 trimers (Castón et al., 2001). Additionally, correct capsid assembly requires a concerted interaction between the precursor and mature VP2 with the inner capsid protein VP3 (Castón et al., 2001; Maraver et al., 2003). The

* Corresponding author. Departamento de Biología Molecular y Celular, Centro Nacional de Biotecnología, Cantoblanco, 28049 Madrid, Spain. Fax: +34-91-5854506.
E-mail address: jfrodrig@cnb.uam.es (J.F. Rodríguez).
[1] Present address: Bionostra S.A., Ronda de Poniente 4, 28760 Tres Cantos, Madrid, Spain.
[2] Present address: Skirball Institute of Biomolecular Medicine, New York University Medical Center, 540 First Avenue, New York, NY 10016.

0042-6822/$ - see front matter © 2004 Elsevier Inc. All rights reserved.
doi:10.1016/j.virol.2004.01.025

interaction of VP3 with the surface capsid VP2 is a key step for IBDV assembly. Failure of classical approaches, such us immunoprecipitation and yeast two-hybrid systems (Tacken et al., 2000, 2003), to detect VP2–VP3 complexes has hampered the progress on this subject. Data presented here demonstrate that VP3 colocalizes exclusively with the pVP2 precursor, thus showing that pVP2CTD plays a key regulatory role within the IBDV assembly pathway. Additionally, we show for the first time that simultaneous expression of two independent genes encoding the pVP2 and VP3 polypeptides leads to formation of virus-like particles (VLPs).

Results

VP3 interacts with the precursor but not with the mature form of the VP2 polypeptide

We sought to analyze the ability of pVP2 and VP2 to interact in vivo with the inner capsid protein VP3. Three previously described recombinant baculoviruses (rBVs), namely FB/his-VP3 (Kochan et al., 2003), FB/pVP2, and FB/VP2 (Martínez-Torrecuadrada et al., 2000) were used for these experiments. Insect cells were grown on coverslips and independently infected with each rBV, or subjected to double infections with FB/his-VP3 + FB/pVP2 or FB/his-VP3 + FB/VP2. At 40 h postinfection (pi), cells were fixed, incubated with sera anti-VP2 and -VP3, and processed for confocal laser scanning microscopy (CLSM).

When independently expressed, the three structural polypeptides display distinctive distribution patterns: (i) VP2 is homogeneously distributed throughout the cytoplasm (Fig. 1A, panel i); (ii) pVP2 forms fine granules interspersed with needle-like formations (Fig. 1A, panel ii); and (iii) VP3 produces discrete ring-like accumulations surrounding the cell nuclei (Fig. 1A, panel iii). Coexpression of VP2 and VP3 does not alter the characteristic distribution patterns of these polypeptides (Fig. 1B, panels i–iii). In contrast, pVP2–VP3 coexpression dramatically modifies the pVP2 pattern. The typical pVP2 granular distribution is replaced

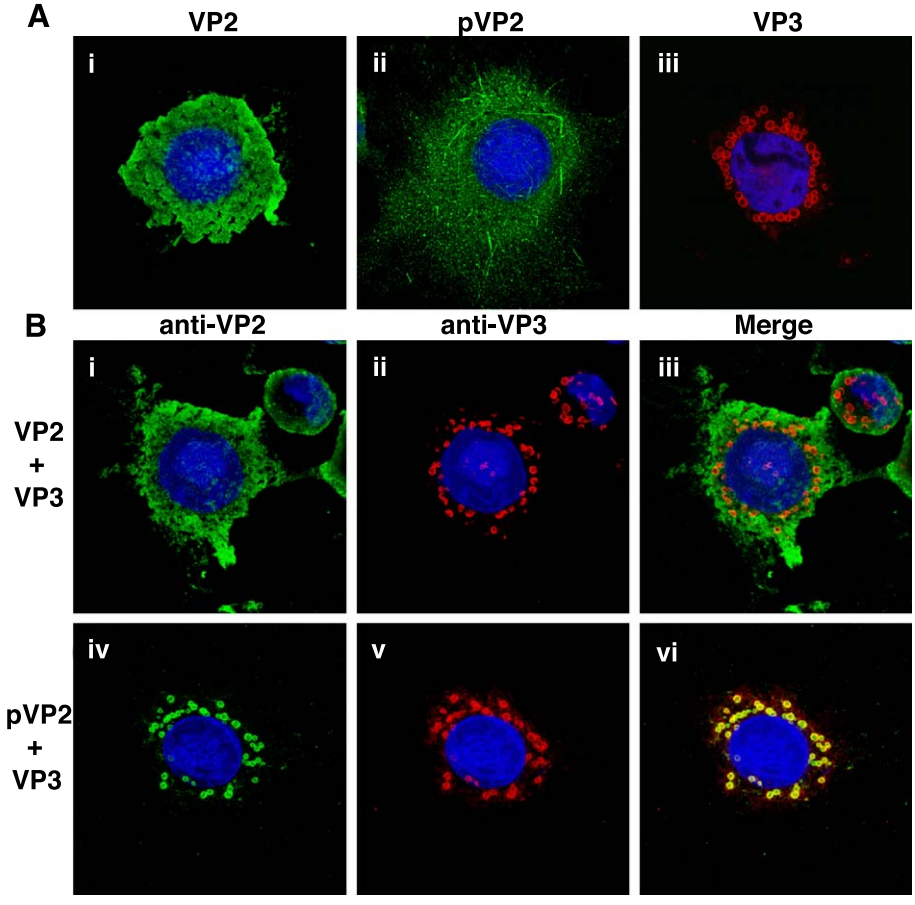

Fig. 1. Effect of VP3 expression on the subcellular distribution of the precursor, pVP2, and mature, VP2, forms of the external capsid IBDV polypeptide. (A) Subcellular distribution of the VP2 (panel i), pVP2 (panel ii), and his-VP3 (panel iii) polypeptides when independently expressed in insect cells. Infected cultures were processed for CLSM using specific antibodies. Green (Alexa 488) corresponds to VP2 and pVP2, and Red (Alexa 594) corresponds to VP3. Blue signal (ToPro-3) corresponds nuclear staining. (B) Subcellular distribution in coinfected cells. Cells were coinfected with rBVs expressing VP2 + his-VP3 or pVP2 + his-VP3. Panels i and iv show green fluorescent signals corresponding to anti-VP2 superimposed to the ToPro-3 signal. Panels ii and v show fluorescent signals corresponding to anti-VP2 superimposed to the ToPro-3 signal. Panels iii and vi show the overlay of the three fluorescent signals.

by accumulation of the pVP2 fluorescent signal into ring-like formations (Fig. 1B, panels iv and vi). These formations are also stained with VP3-specific serum (Fig. 1B, panels v and vi). Taken together, these results suggest that VP3 interacts with the pVP2 precursor but not with the mature form of the protein VP2.

pVP2–VP3 coexpression leads to formation of IBDV-like structures

The results described above prompted a further characterization of the pVP2–VP3 interaction using an alternative approach. Hence, cells were coinfected with either FB/pVP2 + FB/his-VP3 or FB/VP2 + FB/his-VP3. At 40 h pi, cells were fixed and processed for immunoelectron microscopy (IEM) using anti-VP2 or -VP3 specific sera. As controls for this experiment, cells infected with FB/his-VP3, FB/VP2, or FB/pVP2, respectively, were also analyzed.

As assessed by sucrose gradient purification, infection with FB/VP2 and FB/pVP2 leads to formation of 23-nm capsid-like and flexible tubular structures, respectively (Fig. 2A). However, under the experimental conditions used in this analysis, these structures were not detectable by transmission electron microscopy (EM) of thin sections. EM observation of FB/his-VP3-infected cells showed the presence of numerous electron-dense aggregates within the cell cytoplasm (Fig. 2A). These aggregates were not found in cells infected with

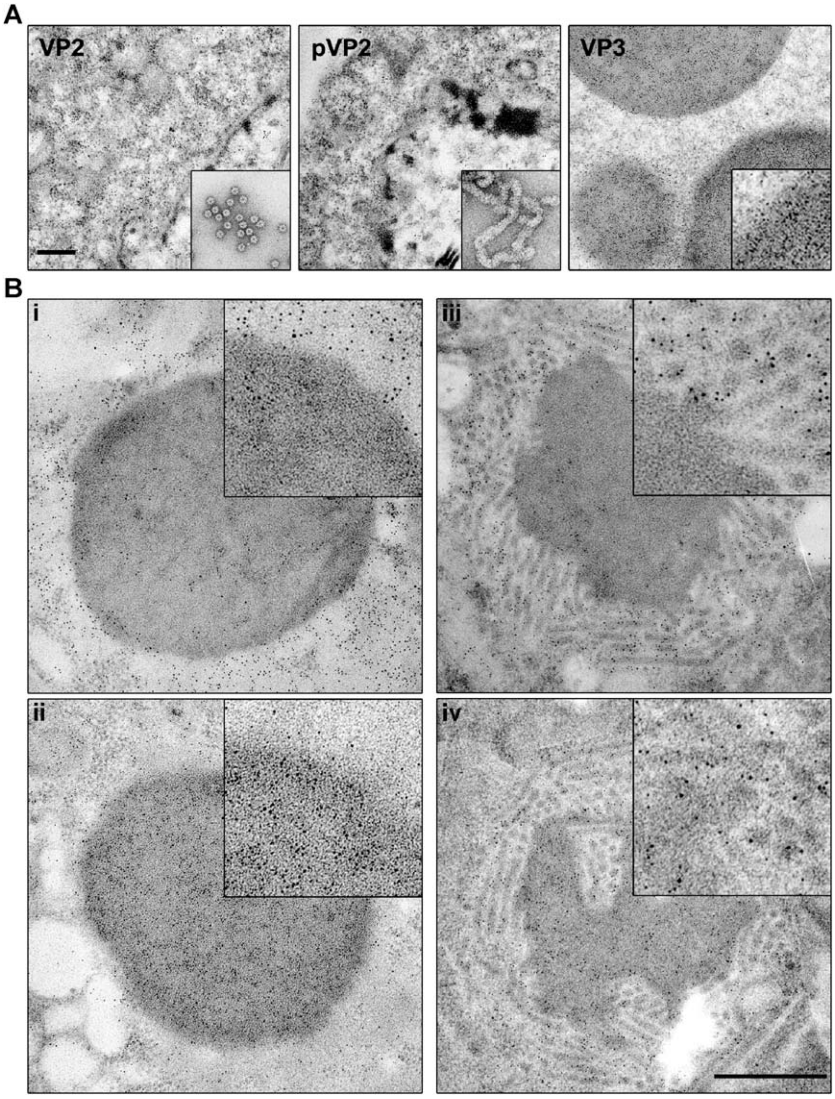

Fig. 2. Detection of intracellular IBDV-like assemblages by EM. (A) Ultrathin sections of H5 cells coinfected with rBVs expressing the VP2, pVP2, and his-VP3 polypeptides, respectively. The specimens were incubated with either rabbit anti-VP2 or -VP3 sera, followed by incubation with goat anti-rabbit Ig conjugated to 5-nm colloidal gold. Inlets in panels corresponding to VP2 and pVP2 specimens correspond to negatively stained IBDV-like assemblages purified from FB/VP2- and FB/pVP2-infected cells. The inlet in panel VP3 shows a higher magnification (×3) detail of a VP3-aggregate. Scale bar indicates 250 nm. (B) Ultrathin sections of H5 cells coinfected with rBVs coexpressing VP2 + his-VP3 (panels i and ii) or pVP2 + his-VP3 (panels iii and iv). The specimens were incubated with either rabbit anti-VP2 or -VP3 sera, followed by incubation with goat anti-rabbit Ig conjugated to 5-nm colloidal gold. Inlets show higher magnification (×3) details of the original images. Scale bar indicates 500 nm.

wild-type FB virus (data not shown). In agreement with previous LSCM data showing the presence of large VP3 accretions in FB/his-VP3-infected cells (Fig. 1A, panel iii), these aggregates were heavily stained with anti-VP3 serum.

Electron-dense aggregates were also detected in cells coinfected with FB/VP2 + FB/his-VP3 (Fig. 2B, panels i and ii). The anti-VP3 strongly recognized these amorphous aggregates while giving a weak cytoplasmic signal (Fig. 2B, panel ii). In contrast, the anti-VP2 serum produced a strong cytoplasmic staining while faintly staining the VP3 aggregates (Fig. 2B, panel i). These results confirmed previous LSCM, and further support the notion that the under these conditions the VP2 and VP3 polypeptides do not colocalize.

As shown in Fig. 2B, panels iii and iv, the cytoplasm of cells coinfected with FB/pVP2 + FB/his-VP3 contained numerous accumulations formed by a mixture of tubules and capsid-like assemblages that, in most cases, enwrap irregularly shaped accretions. The anti-VP3 serum recognized the aggregates as well as the surrounding structures (Fig. 2B, panel iv). On the contrary, the VP2-specific serum strongly recognized both the tubular and capsid-like assemblages while giving a weak staining on the electron-dense accretions (Fig. 2B, panel iii).

Taken together, these results demonstrate that VP3 colocalizes with the pVP2 precursor but not with the mature VP2 polypeptide. Additionally, EM observations showed that pVP2–VP3 coexpression leads to formation of assemblages that strongly resemble those found in cells infected with IBDV or vT7 Poly, a recombinant vaccinia virus (rVV) expressing the IBDV polyprotein (Fig. 3).

VLP assembly in cells coexpressing pVP2 and VP3 from independent genes

The results of the IEM analysis strongly suggested that pVP2–VP3 coexpression might lead to formation of VLP. To investigate this possibility, H5 cultures were coinfected with either FB/pVP2 + FB/his-VP3 or FB/VP2 + FB/his-VP3. At 30 h pi, cells were harvested, homogenized, and used for VLP purification in sucrose density gradients. Gradient fractions were negatively stained and analyzed by transmission electron microscopy. Two different IBDV-like assemblies were detected in samples corresponding to FB/pVP2 + FB/his-VP3-infected cells: (i) type I rigid tubules in fractions close to the bottom of the gradient (not shown); and (ii) 65–70 nm VLP, detected in the middle and upper gradient fractions (Fig. 4A). The purified VLPs are morphologically undistinguishable from

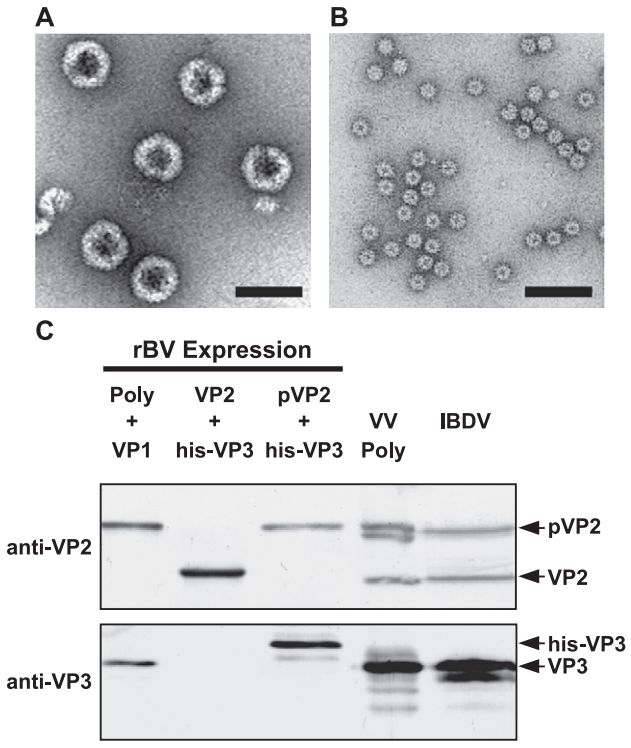

Fig. 4. Characterization of IBDV-like assemblages. (A) EM image of negatively stained VLP purified from H5 cells coexpressing the pVP2 and his-VP3 polypeptides. Scale bar indicates 100 nm. (B) EM image of negatively stained capsid-like structures purified from H5 insect cells coexpressing the VP2 and his-VP3 polypeptides. Scale bar indicates 100 nm. (C) Western blot analysis of IBDV-like assemblages. Samples corresponding to VLP produced in H5 cells infected with the rBV FBD/Poly-VP1 (Poly + VP1), 23-nm capsid-like structures produced in H5 cells coinfected with the rBVs FB/VP2 + FB/his-VP3 (VP2 + VP3), VLP purified from H5 insect cells infected with FB/pVP2 + FB/his-VP3 (pVP2 + VP3), VLP produced in mammalian cells infected with the rVV vT7/Poly (VV Poly), and purified IBDV (IBDV), were analyzed by Western blot using rabbit anti-VP2 and -VP3 antisera, respectively.

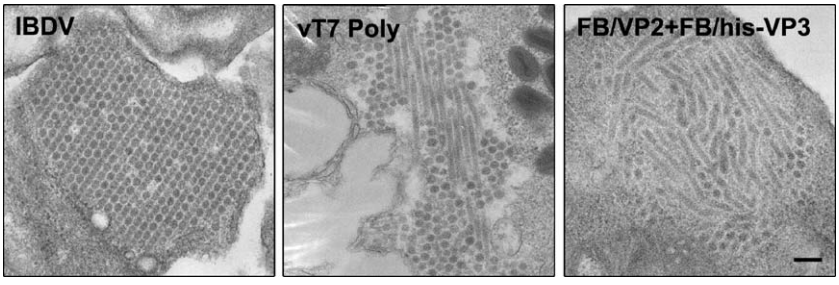

Fig. 3. Detection of IBDV assemblages formed in different systems. EM images correspond to chicken embryo fibroblast infected with IBDV, BSC-1 cells infected the rVV virus vT7 Poly that expresses de IBDV polyprotein, and H5 cells coinfected with FB/pVP2 + FB/his-VP3, respectively. Scale bar indicates 250 nm.

those previously obtained after polyprotein expression in mammalian or insect cells (Fernández-Arias et al., 1998; Maraver et al., 2003). The only assemblage detected in samples corresponding to FB/VP2 + FB/his-VP3-coinfected cells consisted on 23-nm capsid-like structures (Fig. 4B) identical to those previously found in H5 cells expressing the VP2 polypeptide (Castón et al., 2001). The polypeptide profiles of VLP purified from H5 cells coinfected FB/pVP2 + FB/his-VP3, and 23-nm capsid-like assemblages were compared to those of purified IBDV, VLP generated either in mammalian cells infected with the rVV VT7Lac/Poly or in insect cells infected with the rBV FBD/Poly-VP1. Samples were subjected to SDS-PAGE followed by Western blot using anti-VP2 and -VP3 sera. The results obtained are shown in Fig. 4C. An immunoreactive band of 54 kDa, corresponding to pVP2, was detected in all samples except in that from VP2/his-VP3-coexpressing cells. Significant amounts of VP2 (48 kDa) were only detectable in samples corresponding to 23-nm assemblages, IBDV particles, and VLP produced in mammalian cells. The VP3 polypeptide was detected in all samples, except in that corresponding to 23-nm assemblages. The different electrophoretic mobility of the VP3 product detected in VLP purified from pVP2/his-VP3-coexpressing cells reflects the presence of the 3-kDa 6xhis tag at the N-terminus of the his-VP3 polypeptide.

These results demonstrate that simultaneous expression of the pVP2 and VP3 ORFs, driven by independent promoters, allows the assembly of IBDV-like structures including type I tubules and VLP. It is also noteworthy that the fusion of the 6xhis tag to the VP3 N-terminal end does not prevent VLP assembly. This finding provides a new putative target site for the insertion of foreign polypeptide sequences to generate chimerical IBDV VLP.

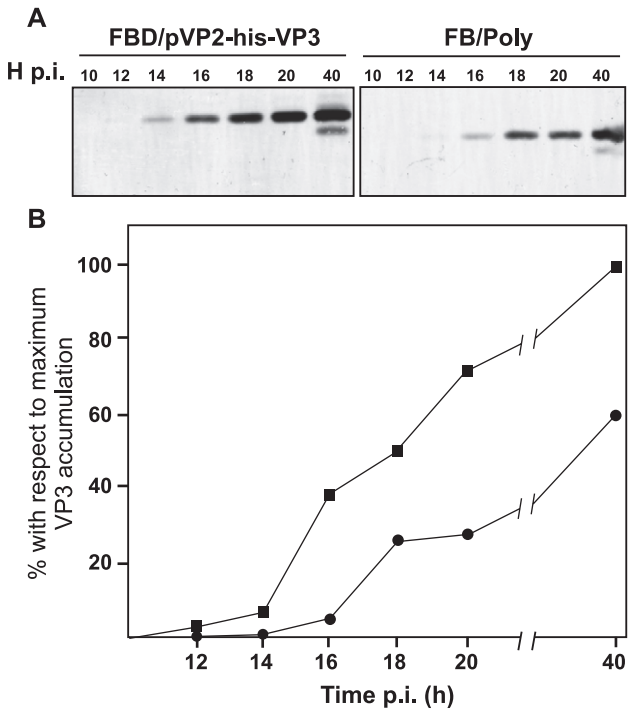

Fig. 5. Comparative analysis of VP3 accumulation rates in insect cells expressing the polyprotein gene or coexpressing the pVP2 and his-VP3 from independent recombinant genes. H5 cell monolayers grown in 24-multiwell plates were infected with either FB/Poly or FBD/pVP2-his-VP3. (A) At the indicated times pi, cells extracts were analyzed by SDS-PAGE and Western blot analysis using rabbit anti-VP3 antiserum. (B) Densitometric analysis. The filter was scanned, and the integrated density of each band determined using the NIH image software. The graph shows the relative VP3 accumulation in samples corresponding from cells infected with FB/Poly (●) or FBD/pVP2-his-VP3 (■) with respect to the maximum accumulation value.

Expression from independent ORFs enhances pVP2 and VP3 accumulation

LSCM data suggested that pVP2–VP3 accumulation was higher in cells coexpressing these polypeptides from independent genes than in those expressing the complete polyprotein (data not shown). To further assess this possibility, a comparative time-course expression analysis was carried out. To facilitate this study, a dual rBV, FBD/pVP2-his-VP3, was constructed. FBD/pVP2-his-VP3 contains the pVP2 and the his-VP3 ORFs under the control of the BV polyhedrin and p10 promoters, respectively. Infection of H5 cells with FBD/pVP2-his-VP3 also leads to formation of IBDV VLP (data not shown). Monolayers of H5 cells were infected with either FB/Poly or FBD/pVP2-his-VP3 at an MOI of 5 PFU/cell. At different times pi, cells were harvested, and the corresponding lysates subjected to SDS-PAGE and Western blot using anti-VP3 serum. After immunostaining (Fig. 5A), filters were analyzed by densitometry and the relative VP3 accumulation at the different time points compared. The results obtained (Fig. 5B) demonstrate that VP3 accumulation is approximately 2-fold higher in FBD/pVP2-his-VP3-infected cells than in those infected with FB/Poly. Almost identical results were obtained with the pVP2 polypeptide (data not shown).

Discussion

IBDV assembly pathway

The results presented demonstrate that pVP2–VP3 coexpression leads to colocalization, unambiguously detectable both by CLSM and IEM. Furthermore, this interaction results in the formation of structures, type I tubules and VLP, akin to those detected in cells infected either with recombinant virus vectors expressing the complete polyprotein or with IBDV (Fernández-Arias et al., 1998; Granzow et al., 1997). In contrast, the presence of VP2–VP3 complexes was not detected in cells simultaneously expressing these polypeptides. Indeed, purification of IBDV-like assemblages from these cultures exclusively rendered 23-nm capsid-like structures identical to $T = 1$ capsid-like structures produced in cells expressing VP2 individually.

The results described demonstrate that pVP2-CTD plays an essential role in the establishment of pVP2–VP3 complexes. At this time, it is not feasible to ascertain whether pVP2-CTD, either alone or in cooperation with other protein domain(s), (i) directly interacts with VP3 or (ii) regulates the establishment of pVP2 homotopic interactions, thus allowing the formation pVP2 complexes with a conformation that allows the subsequent docking of VP3 subunits. Experiments to gain a better understanding on this matter are in progress.

In this report, we provide the first experimental evidence showing that the minimal information required for IBDV capsid assembly is contained within the pVP2 and VP3 polypeptides. Our data indicate that both pVP2 and VP3 acquire a functional conformation when expressed out of the polyprotein context. This is in agreement with previous observations suggesting that polyprotein processing is co-translational (Kibenge et al., 1988), and suggests that, as it has been shown for the Semliky forest virus polyprotein (Nicola et al., 1999), the IBDV polyprotein domains acquire their native folding co-translationally. Our results suggest the hypothesis that the IBDV capsid assembly pathway is initiated after the primary polyprotein processing event that releases pVP2, VP4, and VP3. According to this hypothesis, pVP2 and VP3 would form an immature procapsid, similar to those found during the assembly of other RNA viruses, that is, retro, noda, tetra viruses (Agrawal and Johnson, 1995; Canady et al., 2000; Freed, 1998; Pringle et al., 2001; Zlotnick et al., 1994). It is exciting to speculate that VLP described here, lacking mature VP2, might represent an intermediate stage in capsid maturation. Work on the 3D reconstruction of pVP2 + VP3 VLP is in progress. Hopefully, this will allow determining whether they exhibit structural differences with respect to native virus particles.

IBDV VLP assembly in insect cells

We have recently shown that the VP3 polypeptide expressed in insect cells undergoes a C-terminal proteolytic cleavage that results in the accumulation of a functionally inactive VP3 product lacking 13-aa residues. Consequently, expression of the IBDV polyprotein in insect cells leads, almost exclusively, to the assembly of rigid type I IBDV tubules (Chevalier et al., 2002; Martínez-Torrecuadrada et al., 2000). Hence, detection of VLP in H5 cells coexpressing pVP2 and VP3 was somewhat unexpected. The reasons for the observed improvement on VLP accumulation remain unclear. VP3 proteolytic trimming begins to be noticeable after 24 h pi, before detectable VLP levels have been accumulated in cells expressing the complete polyprotein (Maraver et al., 2003). It seems feasible that the improvement on VLP production detected in insect cells coexpressing the pVP2 and VP3 genes might be at least partially due to the detected increase on pVP2–VP3 accumulation. Alternatively, expression of pVP2 and VP3 from independent genes might facilitate the establishment of pVP2–VP3 interactions leading to a more efficient VLP assembly.

Materials and methods

Cells and viruses

rBVs FB/pVP2, FB/VP2, FB/his-VP3, and FBD/Poly-VP1 have been previously described (Kochan et al., 2003; Maraver et al., 2003; Martínez-Torrecuadrada et al., 2000). Construction of FBD/pVP2-his-VP3 is described below. rBVs were grown and titrated in *Spodoptera frugiperda* H5 insect cells (Invitrogen) as described before (Maraver et al., 2003). The rVV vT7/Poly (Fernández-Arias et al., 1998) was grown and titrated in BSC-1 cells (American Type Culture Collection) as previously described (Lombardo et al., 1999). The IBDV Soroa strain was propagated in chicken embryo fibroblast as previously described (Lombardo et al., 1999).

Construction of FBD/pVP2-his-VP3

A DNA fragment containing the pVP2 coding sequence, nucleotides 1–1536 of the polyprotein ORF, fused to an artificial stop codon was generated by PCR. The reaction was carried out using the plasmid pVOTE.2/POLY (Fernández-Arias et al., 1998) as template and the oligonucleotides 5′-GCGCAGATCTATGACAAACCTGTCAGATCAAACCC and 5′-GCGCAAGCTTAGGCGAGAGTCAGCTGCCTTATGC as primers. The resulting fragment was digested with *Bgl*II and *Hin*dIII, and inserted into the plasmid pFBDual (Invitrogen) previously digested with *Bam*HI and *Hin*dIII, generating the plasmid pFBD/pVP2. Thereafter, a fragment containing the his-VP3 ORF was obtained by digesting the pFB/his-VP3 (Kochan et al., 2003) with *Rsr*II followed by Klenow treatment and *Kpn*I digestion. This DNA fragment was purified and cloned into pFBD/pVP2 previously digested with *Sma*I and *Kpn*I. The resulting plasmid, pFBD/pVP2-his-VP3, contains the pVP2 and his-VP3 ORFs under the control of the polyhedrine and p10 promoters, respectively. The corresponding rBV, FBD/pVP2-his-VP3, was generated using the Bac-to-Bac system following the manufacturers' instructions (Invitrogen).

Purification of IBDV-like structures

H5 cells were subjected to single (5 PFU/cell) or double (5 PFU of each rBV/cell) infections with the appropriate rBVs. At 30 h pi, cells were harvested, lysed, and processed by sucrose gradient sedimentation as described previously (Lombardo et al., 1999). Purification of IBDV particles and vT7/Poly-derived VLP was carried out using cultures of BSC-1 cells as previously described (Lombardo et al., 1999).

Electron microscopy

Samples from sucrose gradient sedimentation were dialyzed against 40 mM Pipes, pH 6.2; 150 mM NaCl. After dialysis, samples were applied to glow-discharged carbon-

coated grids for 1 min and negatively stained with 2% aqueous uranyl acetate for 1 min. IEM was carried out on infected H5 cells. At 40 h pi, H5 monolayers were fixed in situ with 4% paraformaldehyde 0.1% glutaraldehyde in PBS at 4 °C for 4 h. After fixation, cell pellets were resuspended in glycerol and frozen in liquid ethane. Frozen specimens were transferred to a Riechert-Jung AFS freeze-substitution unit (Leika) and maintained at −90 °C in a mixture of methanol and 0.5% (wt/vol) uranyl acetate for 48 h. Thereafter, samples were infiltrated in Lowicryl KYM (EML laboratories) at 30 °C. Polymerization was induced with UV light. Ultrathin sections of the samples were immunolabelled with anti-VP2 or -VP3 rabbit sera followed by incubation with goat anti-rabbit Ig conjugated to 5-nm colloidal gold. Micrographs were recorded with a Jeol 1200 EXII electron microscope operating at 100 kV.

SDS-PAGE and Western blotting

Protein extracts were resuspended in Laemmli's sample buffer and heated at 100 °C for 5 min. Electrophoreses were performed on 12% polyacrylamide gels. Western blot analyses were carried out using anti-VP2 and -VP3 specific rabbit sera as previously described (Fernández-Arias et al., 1998). After immunostaining, nitrocellulose filters were scanned with a UMAX PowerLook 2000 scanner (Umax Systems GmbH). Densitometric analyses were performed using the NIH Image program developed at the U.S. National Institutes of Health (http://rsb.info.nih.gov/nih-image/).

Confocal laser scanning microscopy

H5 cells seeded onto glass coverslips were subjected to either single (5 PFU/cell) or double infections (5 PFU of each rBV/cell) with the indicated rBVs. Monolayers of H5 insect cells were infected with rBVs expressing VP2, pVP2, or his-VP3. At 40 h pi, cells were fixed, incubated with rabbit anti-VP2 and rat anti-VP3 specific sera, followed by incubation with goat anti-rabbit Ig coupled to Alexa 488 (green) and goat anti-rat Ig coupled to Alexa 594 (red). Cell nuclei were stained with ToPro-3. Fluorescent signals detected by CLSM were recorded separately by using appropriate filters. Samples were visualized by epifluorescence using a Zeiss Axiovert 200 microscope equipped with a Bio-Rad Radiance 2100 confocal system. Images were captured using the Laser Sharp software package (Bio-Rad).

Acknowledgments

This work was supported by grants BIO-2000-0905 from Ministerio de Ciencia y Tecnología, and 09/0043/2001 and 07B/0041/2002 from Subdirección General de Investigación of Comunidad Autónoma de Madrid. JRC was supported by the Ramón y Cajal Program from Ministerio de Ciencia y Tecnología. A.O. and F.A. were recipients of fellowships from Comunidad Autónoma de Madrid. We are grateful to the technical assistance provided by the CNB Electron Microscopy, Confocal Laser Scanning Microscopy, and Photography Services.

References

Agrawal, D.K., Johnson, J.E., 1995. Assembly of the T = 4 Nudaurelia capensis omega virus capsid protein, post-translational cleavage, and specific encapsidation of its mRNA in a baculovirus expression system. Virology 207, 89–97.

Böttcher, B., Kiselev, N.A., Stel'Mashchuk, V.Y., Perevozchikova, N.A., Borisov, V., Crowther, R.A., 1997. Three-dimensional structure of infectious bursal disease virus determined by electron cryomicroscopy. J. Virol. 71, 325–330.

Canady, M.A., Tihova, M., Hanzlik, T.N., Johnson, J.E., Yeager, M., 2000. Large conformational changes in the maturation of a simple RNA virus, nudaurelia capensis ω virus (NωV). J. Mol. Biol. 299, 573–584.

Castón, J.R., Martínez-Torrecuadrada, J.L., Maraver, A., Lombardo, E., Rodríguez, J.F., Casal, J.I., Carrascosa, J.L., 2001. C terminus of infectious bursal disease virus major capsid protein VP2 is involved in definition of the t number for capsid assembly. J. Virol. 75, 10815–10828.

Chevalier, C., Lepault, J., Erk, I., Da Costa, B., Delmas, B., 2002. The maturation process of pVP2 requires assembly of infectious bursal disease virus capsids. J. Virol. 76, 2384–2392.

Da Costa, B., Chevalier, C., Henry, C., Huet, J.C., Petit, S., Lepault, J., Boot, H., Delmas, B., 2002. The capsid of infectious bursal disease virus contains several small peptides arising from the maturation process of pVP2. J. Virol. 76, 2393–2402.

Fernández-Arias, A., Risco, C., Martínez, S., Albar, J.P., Rodríguez, J.F., 1998. Expression of ORF A1 of infectious bursal disease virus infectious bursal disease virus results in the formation of virus-like particles. J. Gen. Virol. 79, 1047–1054.

Freed, E.O., 1998. HIV-1 gag proteins: diverse functions in the virus life cycle. Virology 251, 1–15.

Gorbalenya, A.E., Kooning, E.V., 1988. Birnavirus RNA polymerase is related to polymerases of positive strand RNA viruses. Nucleic Acids Res. 16, 7735.

Granzow, H., Birghan, C., Mettenleiter, T.C., Beyer, J., Kollner, B., Mundt, E., 1997. A second form of infectious bursal disease virus-associated tubule contains VP4. J. Virol. 71, 8879–8885.

Kibenge, F.S., Dhillon, A.S., Russell, R.G., 1988. Biochemistry and immunology of infectious bursal disease virus. J. Gen. Virol. 69, 1757–1775.

Kochan, G., González, D., Rodríguez, J.F., 2003. Characterization of the RNA binding activity of VP3, a major structural protein of IBDV. Arch. Virol. 148, 723–744.

Leong, J.C., Brown, D., Dobos, P., Kilbenge, F.S.B., Ludert, J.E., Müller, H., Nicholson, B., 2000. Family *Birnaviridae*. In: Van Regenmortel, M.H.V., Faquet, C.M., Bishop, D.H.L., Carstens, E.B., Estes, M.K., Lemon, S.M., Maniloff, J., Mayo, M.A., McGeoch, D.J., Pringle, C.R., Wickner, R.B. (Eds.), Virus Taxonomy—The Classification and Nomenclature of Viruses: Seventh Report of International Committee on Taxonomy of Viruses. Academic Press, San Diego, pp. 481–490.

Lombardo, E., Maraver, A., Castón, J.R., Rivera, J., Fernández-Arias, A., Serrano, A., Carrascosa, J.L., Rodríguez, J.F., 1999. VP1, the putative RNA-dependent RNA polymerase of infectious bursal disease virus, forms complexes with the capsid protein VP3, leading to efficient encapsidation into virus-like particles. J. Virol. 73, 6973–6983.

Maraver, A., Oña, A., Abaitua, F., González, D., Clemente, R., Diaz-Ruiz, A., Caston, J.R., Pazos, F., Rodríguez, J.F., 2003. The oligomerization

domain of VP3, the scaffolding protein of infectious bursal disease virus, plays a critical role for capsid formation. J. Virol. 77, 6438–6449.

Martínez-Torrecuadrada, J.L., Castón, J.R., Castro, M., Carrascosa, J.L., Rodríguez, J.F., Casal, J.I., 2000. Different architectures in the assembly of infectious bursal disease virus capsid proteins expressed in insect cells. Virology 278, 322–331.

Müller, H., Nitschke, R., 1987. The two segments of the infectious bursal disease virus genome are circularized by a 90,000-Da protein. Virology 159, 174–177.

Nicola, A.V., Chen, W., Helenius, A., 1999. Co-translational folding of an alphavirus capsid protein in the cytosol of living cells. Nat. Cell Biol. 1, 341–345.

Pringle, F.M., Kalmakoff, J., Ward, V.K., 2001. Analysis of the capsid processing strategy of Thosea asigna virus using baculovirus expression of virus-like particles. J. Gen. Virol. 82, 259–266.

Tacken, M.G., Rottier, P.J., Gielkens, A.L., Peeters, B.P., 2000. Interactions in vivo between the proteins of infectious bursal disease virus: capsid protein VP3. J. Gen. Virol. 81, 209–218.

Tacken, M.G., Van Den Beuken, P.A., Peeters, B.P., Thomas, A.A., Rottier, P.J., Boot, H.J., 2003. Homotypic interactions of the infectious bursal disease virus proteins VP3, pVP2, VP4, and VP5: mapping of the interacting domains. Virology 312, 219–306.

Zlotnick, A., Reddy, V.S., Dasgupta, R., Schneemann, A., Ray Jr., W.J., Rueckert, R.R., Johnson, J.E., 1994. Capsid assembly in a family of animal viruses primes an autoproteolytic maturation that depends on a single aspartic acid residue. J. Biol. Chem. 269, 13680–13684.